

Line-Based Multi-Label Energy Optimization for Fisheye Image Rectification and Calibration

Mi Zhang Jian Yao[†] Menghan Xia Yi Zhang Kai Li Yaping Liu

School of Remote Sensing and Information Engineering, Wuhan University, Hubei, China

[†]EMail: jian.yao@whu.edu.cn

Web: <http://cvrs.whu.edu.cn>

Abstract

Fisheye image rectification and the intrinsic parameters estimation for real scene have been addressed in the literature by using line information on the distorted image. In this paper, we propose an easy implemented fisheye image rectification algorithm with line constrains in the undistorted perspective image plane. We propose a novel Multi-Label Energy Optimization (MLEO) method for detecting and selecting long arcs from line images, from which we can obtain intrinsic parameters of fisheye camera utilizing only three circular arcs. The rectification and calibration framework are presented and long arc detection and selection algorithm have been implemented and tested in simulated and real image. We compare the results on real images with the approaches based on the circular arc detection and evaluate the performance of the algorithm for synthetic method.

1. Introduction

As a basic step for higher level tasks, such as structure from motion [17], visual navigation and SLAM [16], automatic rectification and calibration for metric information from fisheye images are the work which has been under active research in recent years. The efforts have led to a remarkable improvements in this field. For example, various open source omni-directional camera calibration tool boxes have been released¹²³ since the launch of unifying theory for central panoramic system[15].

These tools are either based on 2D or 3D calibration patterns [1, 20] with prior knowledge or the line features manually selected from fisheye image [4]. Recently, some automatic rectification and calibration algorithms for single fisheye image have been proposed [5, 9], which mainly focus on the usage of line information from distort image. In fact,

there is a trend that a variety of features on the fisheye image plane are taken into account and this pose an additional challenge for automatic calibration of omni-directional camera.

Among these methods, a dominant paradigm in rectification and calibration for fisheye image has used plumb-line or line based approach [3, 18]. These approaches compute the image of absolute conic from which they obtain the intrinsic parameters of omni-directional camera. Generally speaking, given at least three conics on fisheye image, the camera intrinsic parameters which are denoted by focal length, image center and aspect ratio are computed from the decomposition of absolute conics.

However, despite its geometric success, the rectification and calibration techniques still suffer from the problem of automatic extraction of conics from fisheye image directly. In order to address the conic extraction issue, several approaches have been proposed. For example, the conic extraction problem is simplified as the circle extraction problem by assuming that the edge segmentations belonging to the same circle have the same distance to the center of the circle [10]. Still a huge number of small arcs that consistent with the same circle could not be correctly merged.

In addition, there are many approaches which try to make full use of the characteristic of lines on unit sphere [6, 23]. That is to say, after the detection of connected edge pixels, they project them on the sphere and verify whether they are restrained by the same great circle. The hough transformation is also used to detect line images and refined by minimizing the orthogonal distances to the conic. However, these approaches suffer from the same limitation as perspective cases such as the computationally expensive and importance of parameters sampling [6].

Further, the conic detection algorithm proposed by [9] avoids computational expensive and detects the circular arcs from fisheye image directly. They extract the connected components from edge image and then find the maximum pixels that belong to the same circle which is defined by three random selected points on the contour. Nevertheless, this approach does not take the problem of merging the s-

¹<http://www.robots.ox.ac.uk/~cmei/Toolbox.html>

²<http://webdiis.unizar.es/~lpuig/DLTOmniCalibration>

³<http://www.isr.uc.pt/~jpbar/CatPack/main.htm>

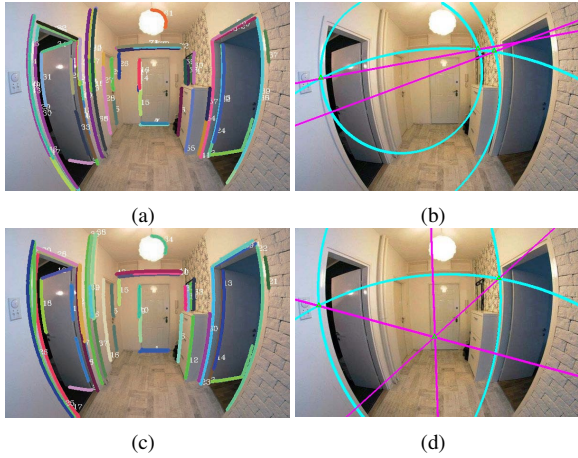


Figure 1. Incorrect estimation of intrinsic parameters due to local minimum estimation of circular arcs: (a) Circular arcs without cluster; (b) Local minimum estimation of circular arcs; (c) Clustered circular arcs; (d) Correct estimation of circular arcs.

small circles that sharing same parameters into consideration. It leads to a local minimum estimation of intrinsic parameters as is shown in Figure 1. Hence many of recent approaches obtain state-of-the-art results by using the linear constrain between the projection on the viewing sphere of a space point and its catadioptric image [21, 22].

Recently, a promising direction for automatic correction and calibration of fisheye image from plumb-lines has emerged with RANSAC technique [11, 18, 14]. Some of these approaches develop a method to extract line-image with 2-points RANSAC and the algorithm is suite for different classes of omnidirectional systems. Another promising technique, the RANSAC Uncapacitated Facility Location (UFL) method [18], simultaneously detect lines in natural images and estimate camera parameters. However, this approach dose not take the problem of automatic selection of the conic arcs and the relationship of detected lines in perspective plane into account. Thus, this method does not work as expected in some situations.

In this paper, we describe an easy implemented approach for fisheye image rectification using the line constrain in undistorted perspective plane. Inspired by the approach proposed in [9, 18, 12, 8, 7], we develop an algorithm to automatic merge and select long circular arcs using the Multi-Labels Energy Optimization (MLEO) method. We also describe a framework for automatic calibration of fisheye camera based on the previous work proposed in [2, 19].

Our approach utilizes a similar arc detection technique proposed in [9] but in different merging and optimizing manner. Instead of simply detecting the arcs of the same contour without considering the similarity between contours, we view the circular arc merging and optimizing process as a multiple labels optimization issue. Each detected

circular arc is regarded as a label that can be represented by circle center and radius while the circular points corresponding to the same label are served as input data. Our approach is motivated by [12], which provides a general model for optimization. In our cases, the data term can be represented by the deviations of each input data to its estimated center (also can be seen as to its corresponding label). And the smooth term can be computed from the euclidean distance between the circle center and the difference of the radius. In addition, we also consider the penalty cost that should be assigned to the label with the assumptions that the circular arcs with small arc length should be merged.

The main difference to [9] is that beside the initial circular arc extraction process, which can be seen as a local circle finding and fitting procedure, we also use Multi-Label Energy Optimization (MLEO) algorithm as the global merging function to fit the long circular arc from the detected circular points. Thus, our approach makes the robust estimation of intrinsic parameters of fisheye image possible.

Unlike the technique proposed in [18], our work deviates this previous work in two aspects. Firstly, our approach uses a general form of energy optimization algorithm which is similar to graph cut like approach to detect the circular arcs on fisheye image. Secondly, we use a simplified fisheye image correction algorithm with line constrains on perspective image plane and derive an algorithm that can automatically select the three properly arranged circular arc which can be further used for intrinsic parameters calibration. The biggest difference is that our automatic circular arc selection algorithm not only consider the relationship between lines in fisheye image plane but also the line relations in perspective plane.

The main contribution of this paper is a pipeline that automatically cluster and select candidate circular arcs for fisheye image rectification and calibration. Unlike the existing technique, our calibration approach also takes the line properties both on fisheye image plane and perspective image plane into consideration. The input is a set of disconnect components from which we automatically extract and cluster the possible circular arcs, and the output is the rectified fisheye image and the corresponding intrinsic parameters (See Figure 2).

For the rectification process, we propose a simplified approach with line constrains which obtain the similar result as the commercial software. While for the calibration procedure, we derive an algorithm that can automatically select three possible long circular arcs for intrinsic parameter estimation. We view the process as a MLEO problem that enables automatically merging and selecting correct contours. This provides an efficient, robust manner of simultaneously clustering the line contours and estimating the camera intrinsic parameters.

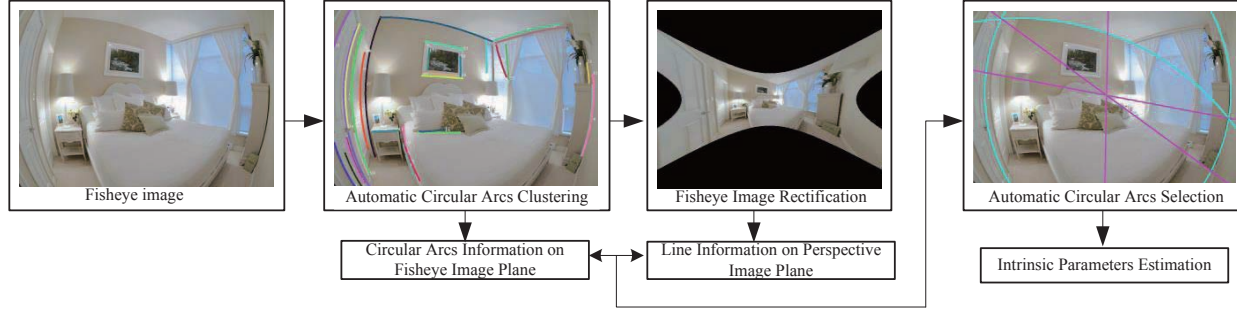


Figure 2. General framework for fisheye image rectification and calibration.

2. Our Approach

In this section, we will introduce an overall framework for rectification and calibration based on the line information (circular arcs) on fisheye image. Given a set of clustered circular arcs, our goal is to rectify the fisheye image and extract the intrinsic parameters from selected circular arcs. This process mainly involves three steps: automatic circular arcs extraction from fisheye image, the image rectification using clustered circular arcs and the intrinsic parameters estimation using selected conics. The general pipeline is illustrated in Figure 2. In our framework, circular arcs are automatically extracted and selected by modelling the problem as a Multi-Label Energy Optimization (MLEO) issue. The clustered circular arcs are then served as the input for fisheye image rectification, resulting in a corrected image on perspective plane. Meanwhile, three candidate circular arcs which are used for intrinsic parameters estimation can be selected in the similar manner. In the selection process, we take not only the circular arcs information on fisheye image plane but also the property of corresponding lines on perspective plane into consideration. Accordingly, this avoids local minimum calibration of intrinsic parameters. Section 3 corresponds to circular arcs extraction and selection procedure for fisheye image rectification and calibration. Section 4 specifies the fisheye image rectification procedure based on line constrained information and section 5 introduces the calibration details using the selected circular arcs.

3. Circular Arcs Extraction and Selection

Suppose that we want to automatically rectify and estimate intrinsic parameters for fisheye image, we should extract and select three candidate circular arcs from it in the first place. It is obvious that the connected components in edge image are the possible candidates. So we start by applying the edge detector such as Canny operator to the fisheye image, followed by using the connected components extraction algorithm in order to obtain possible circular arcs from the edge image. We aim at detecting the circular arcs

ω_i belong to fisheye image plane Π_F that support the label L_c^i which is represented by circle center (cx, cy) and corresponding radius r with minimum energy costs. This can be seen as a circular arc extraction process. Further, in order to automatically select three circular arcs from detected ones, we need to obtain the circular arc $\Omega_j (j = 1 \dots 3)$ on fisheye image plane Π_F with longer radius r_i and their correspond lines $l_j (j = 1 \dots 3)$ should not totally parallel to each other on perspective image plane Π_P . The radius r_i is estimated from the detected circular arcs $\omega_i \in \Pi_F$ and the parallelism which is denoted by line slope k_i is computed from correspond line l_i on perspective image plane (rectified image plane) Π_P . These selected circular arcs ω_i should support possible label L_g^i representing grouped circular arcs. This procedure can be viewed as a circular arc selection process. Following these assumptions, we can model the circular arc clustering and selection problems as an instance of Multi-Label Energy Optimization (MLEO) problem [12, 8, 7].

3.1. Multi-Label Energy Optimization (MLEO) Framework

Given a set of observations P and a finite set of labels L correlated to observations. The graph cut like Multi-Label Energy Optimization (MLEO) problem aims at assigning each observation $p \in P$ a label $f_p \in L$ that joint labelling f minimizes some function $E(f)$. The abstract mathematical form of MLEO function is

$$E(f) = \sum_{p \in P} D_p(f_p) + \sum_{pq \in N} V_{pq}(f_p, f_q) + \sum_{l \in L} h_l \cdot \delta_l(f), \quad (1)$$

where the term $\sum_{p \in P} D_p(f_p)$ denotes the data costs, the term $\sum_{pq \in N} V_{pq}(f_p, f_q)$ represents the smooth costs and the term $\sum_{l \in L} h_l \cdot \delta_l(f)$ means the label costs whose indicator function defined on label set L as

$$\delta_l(f) = \begin{cases} 1 & \exists p : f_p \in L \\ 0 & \text{otherwise} \end{cases} \quad (2)$$

The data term often indicates a standard deviation in the candidate data group and the smooth term often known as a

prior that positively indicates the correlations between observation groups. While the label term gives a penalty to observations meaning that the object function should use as fewer labels as possible.

Our innovation is inspired by this generalized MLEO method, and in the following subsections, we will discuss how this method can be used for circular arcs clustering and selecting in details.

3.2. Circular Arcs Extraction

Assume that the circular arcs $\omega_i \in \Pi_F$ ($i = 1 \dots N$) is the i th detected connect components, which are the possible small arcs to be clustered. Let c_i (c_x^i, c_y^i) and r_i be the corresponding center and radius of i th circular arcs. Our object is to find the minimum number of label L_i that denoted by the parameter (c_x^i, c_y^i) and r_i that fits the given set of circular arcs on fisheye image plane. This can be seen as the Multi-Label Energy Optimization (MLEO) problem. Let s_i^l be the distance between the l th circular point P_l (x_l, y_l) and circular arc center c_i (c_x^i, c_y^i), and c_i^l be the deviation of s_i^l and r_i :

$$s_i^l = \sqrt{(x_l - c_x^i)^2 + (y_l - c_y^i)^2}, \quad (3)$$

$$c_i^l = \|s_i^l - r_i\|. \quad (4)$$

The energy function is denoted as

$$\begin{aligned} E_c(f; \hat{\theta}_c) = & \sum_{i=1}^N \sum_{l=1}^M \|s_i^l - r_i\|^2 + \sum_{i=1}^N \sum_{k=1}^N \|r_i - r_k\| \\ & + \sum_{i=1}^N \sum_{k=1}^N \|c_i - c_k\|^2 + \sum_{i=1}^N \delta_L^i k \left\| \frac{1}{m_i} \right\|^2, \end{aligned} \quad (5)$$

and the optimized parameters in Eq. (5) are:

$$\hat{\theta}_c = \{s_i^l, r_i, c_i, m_i\}, \quad (6)$$

where c_i and c_k represent the center of the circular arcs, m_i is the length of circular arc $\omega_i \in \Pi_F$ and k is the coefficient which is used to augment the penalty cost of the label. The Eq. (5) corresponds to minimization of Eq. (1). Specifically, the data term $d\hat{c}_i^l = \|s_i^l - r_i\|^2$ represents the total deviations of the circular points to its center, the smooth term $sc_i^k = \|r_i - r_k\| + \|c_i - c_k\|^2$ denotes the difference between label L_i ($i = 1 \dots N$) and label L_k ($k = 1 \dots N$), which also represents the difference between different circular arcs parametrized by circle center $c(c_x, c_y)$ and radius r . While the smooth term $lc_i = \delta_L^i k \left\| \frac{1}{m_i} \right\|^2$ regulates the penalty assigned to each circular arc model, meaning the candidate circular arcs with short length should be merged.

This formulated model can also be depicted by Figure 3(a) and Figure 3(b).

These two figures illustrate the graph cut like process correspond to Eq. (5). Given a set of circular points

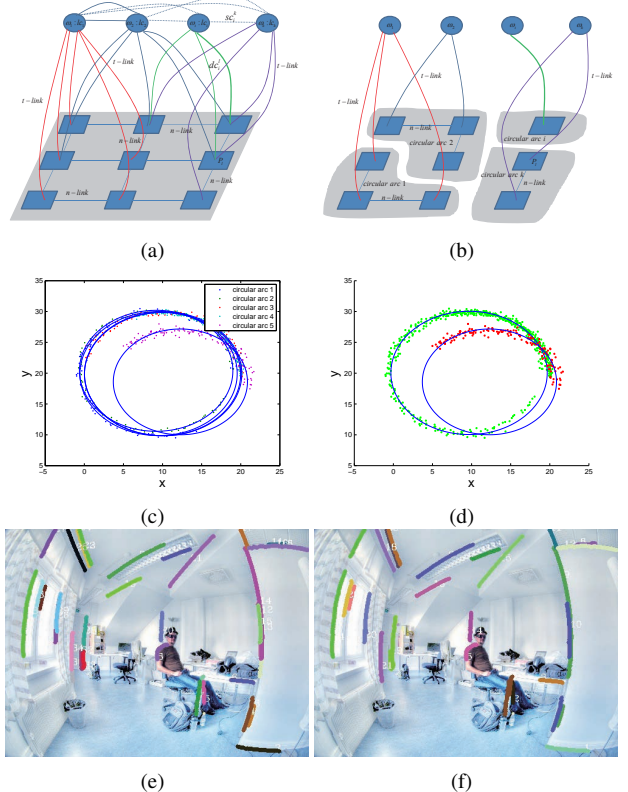


Figure 3. Energy function for optimization: (a) Initial graph corresponding to the terms in Eq. (5); (b) Minimum cut of circular arc after optimization; (c) Initial circular arcs to be clustered for simulated data; (d) Clustered result of simulated data for initial circular arcs; (e) Initial detected circular arcs for fisheye image before clustering. (f) Clustered result for fisheye image.

$P_l(x_l, y_l)$ and a set of circular arcs $\omega_i \in \Pi_F$, each circular point has $n-link$ to its neighbour circular arc points and each circular point also connects to all terminals, namely labels ω_i (the circular arc), with label cost lc_i . In our case, the data term corresponds to the $t-link$ in the graph and the cost of which is $d\hat{c}_i^l$, the smooth term is consistent with the $n-link$ in the graph, which indicates a hidden difference between circular arcs with smooth cost sc_i^k . While the label term adds each potential clustered circular arc ω_i a label cost lc_i . The minimum cut reached until these terms obtaining its local minimum values respectively. This means that all the circular arc points sharing the same circular arc are clustered and the candidate long circular arcs which are used for intrinsic camera calibration are detected. The results with simulated data and real images are illustrated in Figure 3(c)(d) and Figure 3(e)(f). It can be seen that the result of this formulation applied to simulated and real images successfully clustering the circular arc points that belong to the same circle. The shorter circular arcs are correctly detected and clustered and the segmentations sharing the same label (circle center and radius) are identified and merged.

3.3. Circular Arcs Selection

In previous subsection, we propose an algorithm to detect and cluster the circular arcs using the MLEO approach. At the second stage, we need to properly automatically select the three arcs which are served to intrinsic parameters estimation. We formulate the energy function in the similar manner but for different scene. Assuming that the circular arcs $\omega_i \in \Pi_F$ are correctly detected and clustered, our goal is to find three circular arcs $\Omega_j \in \{\omega_i\}_{i=1}^N$ ($j = 1 \dots 3$) which can be used for camera calibration. The main baffle is that the selected circular arcs with their corresponding lines in perspective image plane Π_P should not totally parallel to each other, that is to say, for some lines $l_k \in \Pi_P$ sharing the similar slope k_i need to be given the same label. Further more, the selected circular arcs should be the arcs with longer radius and length in the sense that the arcs deviating from image center should be given more priority. Finally, the distribution of these selected arcs ought to be in different directions on the fisheye image. Based on these assumptions, we formulate Multi-Label Energy Optimization function for the circular arcs selection as

$$E_s(f; \hat{\theta}_s) = \sum_{i=1}^N \sum_{j=1}^4 \ln \gamma (r_i - r_j^p)^2 + \sum_{i=1}^N \sum_{j=1}^4 \ln \beta (k_i - k_j^p)^2 + \sum_{m=1}^4 \sum_{n=1}^4 \lambda \|r_m^p - r_n^p\|, \quad (7)$$

and the parameters in Eq. (7) are:

$$\hat{\theta}_s = \{r_p^j, r_i, k_p^j, k_i\}, \quad (8)$$

where r_j^p and k_j^p represent the predefined radius with respect to fisheye image plane Π_F and slope value with respect to perspective plane Π_P , r_i and k_i denote the radius and slope of candidate circular ω_i on plane Π_F and Π_P respectively, γ , β and λ are the coefficients used for regulating the weights of each term. In Eq. (7), we apply the log like function to data term in order to augment the difference between each selected group. This equation is solved by using the MLEO method mentioned in the previous section.

Four groups could be clustered using the optimization Eq. (7), which takes the three baffles mentioned above into consideration. Each of these four groups contains a set of candidate circular arcs to be selected. To select three circular arcs from these four group, we start by sorting each group according to the length of circular arcs within this group. Four candidate circular arcs can be chosen from the four groups. Again, we sort them by arc length and the final three circular arcs Ω_j ($j = 1 \dots 3$) with longer length are selected from them, which can be served as the circular arcs used for fisheye image intrinsic parameters estimation. Figure 4 illustrates the results of our arc selection algorithm.

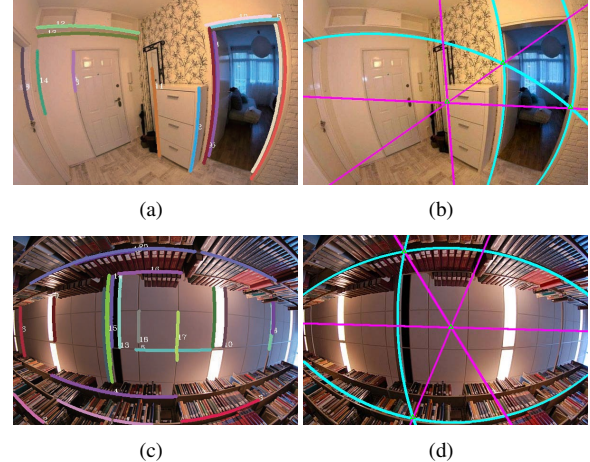


Figure 4. Circular arc selection results: (a) Clustered circular arcs; (b) Selected circular arcs for intrinsic parameter estimation; (c) Clustered circular arcs; (d) Selected circular arcs for intrinsic parameter estimation.

It is obvious that the arcs that can be properly used for intrinsic parameters estimation have been correctly selected.

4. Line-Based Fisheye Image Rectification

The main aim of fisheye image rectification is to transform the distort fisheye image to the so called perspective image plane which preserves the majority of visual effects as we have usually seen. For example, the straight line on the perspective plane has to be straight [13]. We use a simplified spherical projection model with line constrains on perspective plane to automatically transfer the fisheye image to perspective image plane. This model is depicted in Figure 5. Assume that a point $P(X, Y, Z) \in R^3$ lies on a ray through the sphere center O which intersect the sphere on the point M . The fisheye image point which is denoted by $N(x, y)$ can be viewed as the orthogonal projection of point M . The corresponding point $N'(u, v)$ on the perspective plane can be seen as the intersection of the ray that through sphere center and the point P and the plane parallel to fisheye image plane.

The function that maps the distort point N on fisheye image plane Π_F to the corresponding point N' on perspective plane Π_P and its inverse map is:

$$\begin{bmatrix} u \\ v \end{bmatrix} = \frac{z_0}{\sqrt{R^2 - x^2 - y^2}} \begin{bmatrix} x \\ y \end{bmatrix}, \quad (9)$$

$$\begin{bmatrix} x \\ y \end{bmatrix} = \frac{R}{\sqrt{u^2 + v^2 + z_0^2}} \begin{bmatrix} u \\ v \end{bmatrix}, \quad (10)$$

where R is the radius of the sphere, z_0 is the location of perspective plane Π_P that parallel to the fisheye image plane Π_F , (x, y) denotes a point on the plane Π_F and (u, v) represents a point on the plane Π_P .

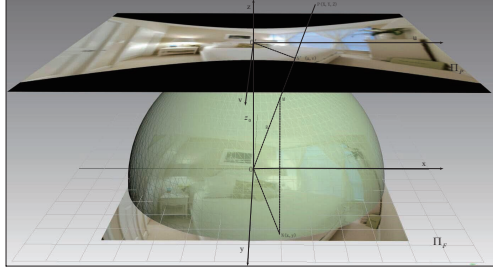


Figure 5. Fisheye image rectification model. The fisheye image point $N(x, y)$ on fisheye image plane Π_F is the orthogonal projection of point M on the sphere, and the point M is the intersection of the ray PO and the sphere. Point $N'(u, v)$ is the corresponding point on perspective image plane Π_P .

This simplified model has the same meaning as the model proposed in [2] in that the camera position denoted by parameter ξ in function $\hbar(x)$ moves to infinite along the z axis. Suppose that a set of circular arcs denoted by $\omega_i \in \Pi_F$ and its corresponding lines denoted by $l_i \in \Pi_P$ in perspective plane. The relationship between the points lie on the circular arcs and corresponding points lie on the lines can be expressed by Eq. (9) and Eq. (10).

Knowing the fact that the straight line in perspective plane remains to be straight, we use the line constrains on perspective plane to denote the possible hidden distortion parameters. That is, when the line on perspective plane keep straight after optimization, the distortion on fisheye image is removed. In fact, the hidden distortion parameters with line constrain in this model are determined by the radius R of the sphere. So the problem of removing distortion is to find the radius R that minimize the weighted deviation of the line in perspective plane. The object function is defined as

$$E(d_i, R) = \sum_{j=1}^n \sum_{i=1}^m w_i \|d_i^j\|^2 = \sum_{j=1}^n \sum_{i=1}^m w_i \left\| \frac{a_i u_j + b_i v_j + c_i}{\sqrt{a_i^2 + b_i^2}} \right\|^2, \quad (11)$$

where d_i is the standard deviation of each line l_i in perspective space, w_i is the weight of line l_i and is in proportion to the length of line l_i , (a_i, b_i, c_i) represents the direction of line l_i in perspective plane and (u_j, v_j) denotes the point lies on line l_i .

Now the object function is fully defined, the parameter R which represents the hidden distortion variable can be estimated as a global minimum:

$$\hat{R} = \operatorname{argmin} E(d_i, R). \quad (12)$$

The minimization is done using the Levenberg-Marquardt (LM) non-linear least square method. Once the optimized parameter \hat{R} is obtained using this non-linear optimization method, the fisheye image is rectified.

5. Line-Based Camera Intrinsic Calibration

In order to give a complete rectification and calibration framework, we will describe briefly about the intrinsic parameters estimation algorithm proposed by [2] from three circular arcs. Assuming that the circular arcs (also can be seen as conics) which are used for intrinsic parameters estimation have been clustered and selected from detected contours, our aim is to find the intrinsic parameters denoted by focal length, image center and aspect ratio.

The main steps involving in catadioptric camera calibration from three circular arcs includes:

- 1) Determine the conics Ω_j ($j = 1 \dots 3$) from selected circular arcs;
- 2) Estimate the point $P(\hat{I}_i, \hat{J}_i)$ ($i = 1 \dots 3$) which is the intersection of polar line and the conic locus;
- 3) Estimate the absolute conic $\hat{\Omega}_\infty$ going through points $P(\hat{I}_i, \hat{J}_i)$ ($i = 1 \dots 3$);
- 4) Perform the Cholesky decomposition of $\hat{\Omega}_\infty$ to estimate the intrinsic matrix K .

Details reasoning and calculation can refer to [3].

6. Experimental Results

We demonstrate the results of our rectification and calibration algorithm on a number of examples, including the fisheye image in real scene and the images download from the Internet. To evaluate the correctness of our algorithm, we make a comparison between our results and the commercial software DxO. Also we verify the standard deviations of lines in perspective image plane between our cluster results and the algorithm proposed in [9] when applying LM optimization algorithm. For the cases where the number of circular arcs extracted from single image are relatively insufficient to estimate intrinsic parameters, we use a synthetic method combining the circular arcs from a variety of images captured by the same fisheye camera. To begin with, we extract the circular arcs with our proposed technique for each fisheye image respectively. Then the synthetic circular arcs (see Figure 10(a)) are utilized for fisheye image rectification. Finally, the three circular arcs selected from synthetic ones are served for intrinsic parameters estimation using the existed algorithm presented in Section 5.

In Figure 6, we illustrate our results and the results using the method mentioned in [9]. It can be seen from Figure 6(d) that the RMS of the clustered circular arcs (our method denoted by red curve) is much smaller than that of the arcs which are not clustered (method in [9] represented by green curve). Also the LM iteration times of our method is relatively short. We also present the results (see

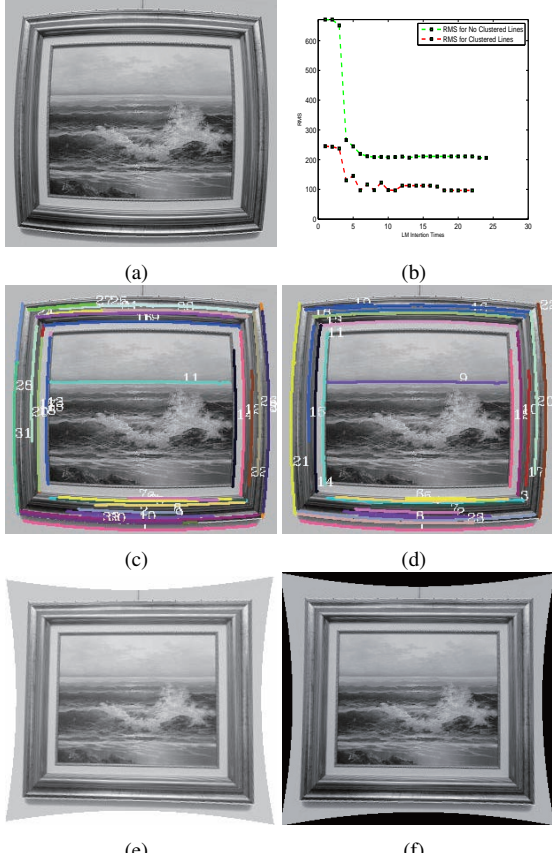


Figure 6. Rectified results of ours and the results using algorithm in [9]: (a) Source fisheye image to be rectified; (b) Root Mean Square (RMS) of our method and the method proposed in [9]. (c) Extracted circular arcs from source image using algorithm proposed in [9]; (d) Extracted and clustered contours from source image using our method. (e) Corrected fisheye image using method proposed in [9]; (f) Rectified fisheye image using our method.

Figure 7) where the method in [9] does not correctly rectified. This is mainly caused by the incorrect detection of circular arcs on the out rings edges. In Figure 8, we compare our automatically rectified results with manually corrected results of commercial software DxO. Our line constrained method produces the similar results as the DxO does. Figure 9 presents the results for images download from the Internet. These rectified Internet images produce the visual effects as we have expected. Our method well preserve the line properties in perspective plane and the straight lines on the rectified image plane remains straight. As the synthetic method mentioned previously, the Figure 10 depicts corresponding results. The circular arcs in different color represent the circular arcs detected in different fisheye image. It can be seen from Figure 10 that the RMS of line deviation of our synthetic method becomes more and more steady with the increasement of synthetic frame number. And the three circular arcs are correctly selected from the synthetic line image using our proposed algorithm. This make sense

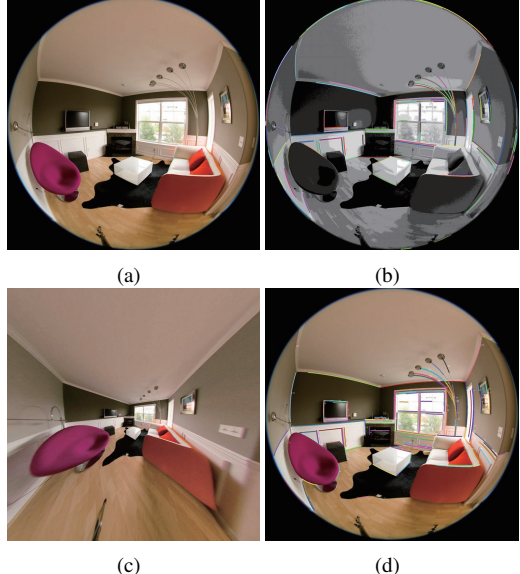


Figure 7. Fisheye image which can not be correctly rectified by algorithm in [9]: (a) Source fisheye image to be rectified; (b) Extracted circular arcs using algorithm proposed in [9]; (c) Rectified fisheye image using our method. (d) Clusters of circular arcs using our algorithm.



Figure 8. Rectified results of ours and the results using DxO: Images in the first row are source images. The middle row are manually rectified results using commercial software DxO. The images depicted in the last row are our automatically rectified results.

for the situation where the line information is infertility on single fisheye image and provide a flexible way for intrinsic parameter estimation.

Further results are shown in the supplementary material.



Figure 9. Rectified results of Internet images: The first row is the source image download from Internet. The second row is the clustered circular arcs using our proposed algorithm. And the last row depicts corresponding rectified results.

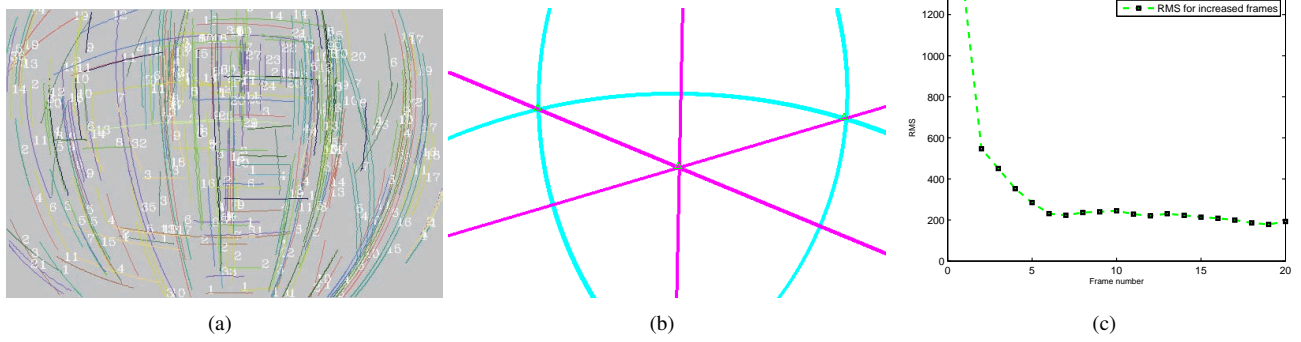


Figure 10. Synthetic method for fisheye image rectification and calibration: (a) Synthetic circular arcs from 20 frame captured by the same fisheye camera; (b) Selected circular arcs used for intrinsic parameter estimation($\gamma = \frac{1}{100}, \beta = 1.0, \lambda = 1.0$); (c) Root mean square (RMS) for increasing number of frame.

The code is implemented in C with OpenCV support and is publicly available for download at author's website⁴.

7. Conclusion

In this paper, we proposed an algorithm for fisheye image rectification and calibration and devise a pipeline based on pump-line approach. Circular arcs are automatically detected and clustered by using MLEO approach. In addition, we present an automatic circular arcs selection algorithm, which considers both the property of lines on perspective image plane and the characteristic of circular arcs on fisheye image plane. Our algorithm is tested in various situations, including fisheye image captured in real scene and images download from Internet. We also make a compar-

ison between our results and existed approaches. Experimental results demonstrate the robustness of our proposed technique. However, there is still limitation that we need to offer a reasonable initial value for Levenberg-Marquardt (LM) iteration process. Future work will focus on this issue and provide a time saving approach for intrinsic parameters estimation from multiple fisheye images captured by the same catadioptric camera.

Acknowledgement

This work was partially supported by the National Basic Research Program of China (Project No. 2012CB719904), the National Natural Science Foundation of China (Project No. 41271431), and the South Wisdom Valley Innovative Research Team Program.

⁴<http://cvrs.whu.edu.cn/projects/FIRC/>

References

- [1] D. Aliaga. Accurate catadioptric calibration for real-time pose estimation in room-size environments. In *ICCV*, 2001. 1
- [2] J. P. Barreto. *General Central Projection Systems Modeling, Calibration And Visual Servoing*. PhD thesis, University of Coimbra, 2003. 2, 6
- [3] J. P. Barreto and H. Araujo. Paracatadioptric camera calibration using lines. In *ICCV*, 2003. 1, 6
- [4] J. P. Barreto and H. Araujo. Geometric properties of central catadioptric line images and their application in calibration. *IEEE Transactions on Pattern Analysis and Machine Intelligence*, 27(8):1327 – 1333, 2005. 1
- [5] J. P. Barreto, J. Roquette, P. Sturm, and F. Fonseca. Automatic camera calibration applied to medical endoscopy. In *BMVC*, 2009. 1
- [6] J. C. Bazin, I. Kweon, C. Demonceaux, and P. Vasseur. Rectangle extraction in catadioptric images. In *ICCV*, 2007. 1
- [7] Y. Boykov and V. Kolmogorov. An experimental comparison of min-cut/max-flow algorithms for energy minimization in vision. *IEEE Transactions on Pattern Analysis and Machine Intelligence*, 26(9):1124 – 1137, 2004. 2, 3
- [8] Y. Boykov, O. Veksler, and R. Zabih. Fast approximate energy minimization via graph cuts. *IEEE Transactions on Pattern Analysis and Machine Intelligence*, 23(11):1222–1239, 2001. 2, 3
- [9] F. Bukhari and M. N. Dailey. Automatic radial distortion estimation from a single image. *Journal of Mathematical Imaging and Vision*, 45(1):31–45, 2013. 1, 2, 6, 7
- [10] C. B. Burchardt and K. Voss. A new algorithm to correct fish-eye- and strong wide-angle-lens-distortion from single images. In *ICIP*, 2001. 1
- [11] J. B. Cameo, G. L. Nicolas, and J. J. Guerrero. A unified framework for line extraction in dioptric and catadioptric cameras. In *ACCV*, 2012. 2
- [12] A. Delong, A. Osokin, H. N. Isack, and Y. Boykov. Fast approximate energy minimization with label costs. *International Journal of Computer Vision*, 96(1):1–27, 2012. 2, 3
- [13] F. Devernay and O. Faugeras. Straight lines have to be straight – automatic calibration and removal of distortion from scenes of structured environments. *Machine Vision and Applications*, 13(1):14–24, 2001. 5
- [14] M. A. Fischler and R. C. Bolles. Random sample consensus: a paradigm for model fitting with applications to image analysis and automated cartography. *Communications of the ACM*, 24(6):381–395, 1981. 2
- [15] C. Geyer and K. Daniilidis. A unifying theory for central panoramic systems and practical implications. In *ECCV*, 2000. 1
- [16] C. Mei. *Laser-Augmented Omnidirectional Vision for 3D Localisation and Mapping*. PhD thesis, INRIA Sophia Antipolis, Project-team ARobAS, 2007. 1
- [17] C. Mei and F. Malis. Fast central catadioptric line extraction, estimation, tracking and structure from motion. In *ICIRS*, 2006. 1
- [18] R. Melo, M. Antunes, J. P. Barreto, G. Falcao, and N. Goncalves. Unsupervised intrinsic calibration from a single frame using a “plumb-line” approach. In *ICCV*, 2013. 1, 2
- [19] L. P. Morales. *Omnidirectional multi-view systems: calibration, features and 3D information*. PhD thesis, Departamento de Informtica e Ingeniera de Sistemas Escuela de Ingeniera y Arquitectura Universidad de Zaragoza, Spain, 2011. 2
- [20] C. Toepfer and T. Ehlgren. A unifying omnidirectional camera model and its applications. In *ICCV*, 2007. 1
- [21] F. C. Wu, F. Duan, Z. Y. Hu, and Y. H. Wu. A new linear algorithm for calibrating central catadioptric cameras. *Pattern Recognition*, 41(10):3166–3172, 2008. 2
- [22] X. H. Ying and Z. Y. Hu. Catadioptric camera calibration using geometric invariants. In *ICCV*, 2003. 2
- [23] X. H. Ying and Z. Y. Hu. Catadioptric line features detection using hough transform. In *ICPR*, 2004. 1